Spin-valley density wave in moiré materials

Constantin Schrade and Liang Fu

Phys. Rev. B **100**, 035413 — Published 10 July 2019

DOI: 10.1103/PhysRevB.100.035413

Spin-valley density wave in moiré materials

Constantin Schrade and Liang Fu
Department of Physics, Massachusetts Institute of Technology, 77 Massachusetts Ave., Cambridge, MA 02139
(Dated: June 19, 2019)

We introduce and study a minimum two-orbital Hubbard model on a triangular lattice, which captures the key features of both the trilayer ABC-stacked graphene-boron nitride heterostructure and twisted transition metal dichalcogenides in a broad parameter range. Our model comprises first- and second-nearest neighbor hoppings with valley-contrasting flux that accounts for trigonal warping in the band structure. For the strong-coupling regime with one electron per site, we derive a spin-orbital exchange Hamiltonian and find the semiclassical ground state to be a spin-valley density wave. We show that a relatively small second-neighbor exchange interaction is sufficient to stabilize the ordered state against quantum fluctuations. Effects of spin- and valley Zeeman fields as well as thermal fluctuations are also examined.

PACS numbers: 68.65.Cd; 68.65.Ac; 71.10.Fd

I. INTRODUCTION

Moiré materials are layered $2d$ crystals in which a lattice mismatch or a rotational misalignment gives rise to a long-period superlattice structure. These moiré superlattices host narrow mini-bands that promise enhanced correlation effects.[1,2] Recent experiments have discovered correlated insulators, superconductivity, orbital ferromagnetism and spontaneous (quantum) Hall effect in several moiré materials including twisted bilayer graphene,[3–9] trilayer ABC-stacked graphene (TG) on hexagonal boron nitride (h-BN),[10–12] and twisted transition metal dichalcogenides (TMDs).[13,14]

A paradigmatic approach for studying such correlated electron phenomena is the Hubbard model. For the aforementioned moiré materials, the effective Hubbard model comprises both spin and orbital degrees of freedom[15–18] arising from the K, K'-valleys of the original Brillouin zone. Since the separation of K, K'-valleys is much larger than the reciprocal vector of the moire superlattice, intervalley hybridization is weak, thus, leading to Hubbard models with emergent symmetries.

A first concrete example are AB-stacked bilayers of TMDs which at small twist angle form a triangular superlattice.[19,20] A recent work[20] has found that the topmost moiré valence bands of this material can be described by a two-orbital Hubbard model where each orbital resides in one of the two layers and electron's spin is locked to the valley. When the small layer separation is neglected, intra- and interlayer Coulomb repulsions are equal, which yields an interaction with SU(4)-symmetry.

A second example is TG/h-BN.[21–28] In this heterostructure, a vertical electric field enables a high degree of band structure tunability and permits the realization of a two-orbital Hubbard model on a triangular lattice[15,16] with valley-contrasting flux.[22–28] This flux breaks SU(4)-symmetry while preserving charge and spin conservation within each valley.

A last example is twisted bilayer graphene where two graphene sheets are stacked with a small twist angle. Theoretical works have constructed manifestly-symmetric, maximally-localized Wannier orbitals[18,29,31] and derived a two-orbital Hubbard model on a honeycomb lattice with extended interactions.[18,29–31] In both TG/h-BN and twisted bilayer graphene, the two orbitals in the effective Hubbard model correspond to Wannier states from the K, K'-valleys.

In this work, we introduce and study a minimum two-orbital Hubbard model on a triangular lattice, which captures key features of both TG/h-BN and twisted TMDs in a broad parameter range. Our model includes first- and second-neighbor (NN) hopping as well as on-site interaction U. The first-NN hopping is complex and has opposite phases for the two valleys accounting for a valley-contrasting flux, while the second-NN hopping is real due to crystal symmetry. Focusing on the large-U limit with one electron per site, we derive a spin-orbital exchange Hamiltonian H_J with SU(2) × SU(2) × U(1)-symmetry, associated with spin and charge conservation within each valley. By solving H_J in the semiclassical limit, we find a "spin-valley density wave" ground state with four-sublattice order. We also show by a spin-wave analysis that a relatively small second-neighbor exchange interaction is sufficient to stabilize the order against quantum fluctuations at zero temperature. We show that thermal melting of the $T = 0$ ground state restores spin rotation symmetry and may lead to a valley density wave state at low temperature, which breaks discrete lattice and time-reversal symmetries. Finally, we examine the effects of spin and valley Zeeman fields and discuss experimental signatures of the predicted density wave states in TG/h-BN and twisted TMD.

II. MODEL

We begin with a detailed description of our proposed Hubbard model for TG/hBN and twisted TMDs.

We will first consider TG/h-BN. In this heterostructure, both individual components, TG and h-BN, have a 1.5%-mismatch of lattice constants which results in a triangular moiré superlattice, see Fig. 1(a). For this su-

perlattice, the microscopic symmetries are time-reversal symmetry, three-fold rotations C_3 around the axis perpendicular to the TG/h-BN sheets and mirror reflection symmetry M.

The mini-band structure in TG/h-BN arises from the moiré potential of h-BN acting on low-energy electrons in TG..[21,23,24] An important experimental parameter for tuning the bandwidth and topology of the mini-bands is the external electric field[10,11] that provides a potential difference between the top and bottom graphene sheets. In TG/hBN, depending on the the sign of the potential difference, the mini-band structure is either in a "Hubbard regime" with zero Chern number[22–26] or in a "Quantum Hall regime" with finite valley Chern number.[12,27,28,32] In this work, we focus on the "Hubbard regime" without Chern number.

The Hubbard regime is realized when electrons in TG are pulled towards h-BN by the external electric field. The resulting mini-band structure can be intuitively understood from the deep potential limit, where each minimum of the moiré potential creates a localized Wannier orbital. Since the potential minima form a triangle lattice, one naturally expects a triangle-lattice tight-binding model for TG/h-BN, as demonstrated by previous band structure calculations.[27,33] Since the hopping matrix elements decay rapidly with the distance, we study a *minimum* model for TG/h-BN that only retains the dominant hopping terms. The full Hamiltonian of our model is $H = H_0 + H_I$, where the single-particle Hamiltonian H_0 is given by,

$$H_0 = \sum_{\alpha} \left(t_1 \sum_{\langle i,j \rangle} e^{i\Phi_\alpha^{ij}} c_{i\alpha}^\dagger c_{j\alpha} + t_2 \sum_{\langle\langle i,j \rangle\rangle} c_{i\alpha}^\dagger c_{j\alpha} + ... \right), \tag{1}$$

where $c_{i\alpha}$ annihilates an electron at site i in state $\alpha = (\sigma, \tau)$ with spin $\sigma = \uparrow, \downarrow$ and orbital $\tau = \pm$ associated with the K, K'-valleys. t_1, t_2 are the dominant hopping amplitudes between first and second-NN sites. The t_1-hoppings are generally complex and carry phases $\Phi_\alpha^{ij} = -\Phi_\alpha^{ji}$, which are independent of spin and opposite for the two valleys. Microscopically, these phases arise from the trigonally warped Dirac dispersions at the K, K'-valleys and are allowed by symmetry. The total flux piercing through each elementary triangle is $3\Phi_\alpha \equiv \Phi_\alpha^{ij} + \Phi_\alpha^{jk} + \Phi_\alpha^{ki}$ where $\Phi_{\sigma,+} = -\Phi_{\sigma,-} \equiv \Phi$ and i, j, k are three consecutive triangle sites along the directed first-NN bonds, see Fig. 1(b). In comparison, the t_2-hoppings are real-valued due to the combination of reflection $x \to -x$ and time-reversal symmetry, which acts within each valley. In this work, the t_2 hopping will play an important role as shown below.

Second, the dominant term in the projected Coulomb interactions onto the narrow mini-bands is the on-site density interaction,

$$H_I = \frac{U}{2} \sum_i (n_i - n_0)^2, \tag{2}$$

where $n_i = \sum_{\sigma,\xi} c_{i\sigma\xi}^\dagger c_{i\sigma\xi}$ is the total number electrons on the i-site, n_0 controls the filling and U is the interaction amplitude. In this work, we will focus on the regime where kinetic exchange due to single-particle hopping dominates over direct interactions between electrons on different sites. We remark that previous works have considered alternative mechanism of SU(4) symmetry breaking due to extended interactions instead of valley-dependent single-particle hopping.[16,26]

III. VARIATIONAL STUDY

We now proceed to study of our two-orbital Hubbard model in the strong-coupling limit, $U \gg t_1, t_2$. Such an approach complements studies in the weak coupling regime[30,34–41] and is a reasonable way towards understanding the real system that may eventually be in an intermediate coupling regime. Specifically, we focus on the filling of one electron per site and, as shown in Appendix A, perform a perturbative expansion to second order in t_1, t_2 leading to a spin-orbital exchange interaction,

$$H_J = \sum_{\alpha,\beta} \left(J_1 \sum_{\langle i,j \rangle} e^{i(\Phi_\beta^{ij} - \Phi_\alpha^{ij})} T_{\beta,i}^\alpha T_{\alpha,j}^\beta + J_2 \sum_{\langle\langle i,j \rangle\rangle} T_{\beta,i}^\alpha T_{\alpha,j}^\beta \right). \tag{3}$$

Here, $J_1 = 2t_1^2/U$, $J_2 = 2t_2^2/U$ are antiferromagnetic exchange couplings and $T_\beta^\alpha = |\beta\rangle\langle\alpha|$ are SU(4) generators that act on the spin-orbital basis states $|+,\uparrow\rangle$, $|+,\downarrow\rangle$, $|-,\uparrow\rangle$, $|-,\downarrow\rangle$. The SU(4) generators satisfy $\sum_\alpha T_\alpha^\alpha = 1$, $(T_\beta^\alpha)^\dagger = T_\alpha^\beta$, $[T_\beta^\alpha, T_{\alpha'}^{\beta'}] = \delta_{\alpha\alpha'} T_\beta^{\beta'} - \delta_{\beta\beta'} T_{\alpha'}^\alpha$. Despite being written in terms of SU(4) generators, H_J is not SU(4) symmetric when $\Phi_\alpha^{ij} \neq 0$, as the exchange of electrons in different orbitals picks up a orbital-dependent phase factor. This phase factor shows up in the first term $\propto J_1$ and leads to a breaking of SU(4) down to SU(2)×SU(2)×U(1)

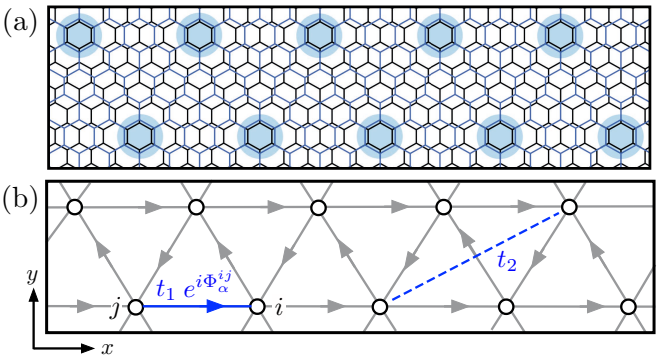

FIG. 1. (Color online) (a) Schematic plot of the triangular moiré superlattice formed by TG (black) and h-BN (blue). (b) Triangular lattice with directed bonds. First-NN hoppings along the bond direction acquire a valley-contrasting phase, $t_1 e^{\Phi_\alpha^{ij}}$. Second-NN hoppings t_2 are real-valued.

with generators $\vec{\sigma}\oplus I$, $I\oplus\vec{\sigma}$, and $I\oplus(-I)$, where σ's are 2×2 Pauli matrices associated with spin and $\oplus$ denotes direct sum of the two valleys.

Next, we will determine the ground states of H_J in the semiclassical approximation. For this purpose, we consider the following product state,

$$|\Psi\rangle = \prod_i \left(\sum_\alpha v_{\alpha,i}\,|\alpha\rangle_i\right), \tag{4}$$

where we have defined complex and normalized vectors $\boldsymbol{v}_i = (v_{1,i}, v_{2,i}, v_{3,i}, v_{4,i})^T$ for each site. To find the variational ground states based on this ansatz, we note that the two terms in the effective Hamiltonian permute the states on first-NN and second-NN sites, $T^\alpha_{\beta,i}T^\beta_{\alpha,j} = |\beta_i,\alpha_j\rangle\langle\alpha_i,\beta_j|$. Hence, as shown in Appendix B, the variational ground states need to minimize,

$$\langle\Psi|H_J|\Psi\rangle = J_1\sum_{\langle i,j\rangle}\left|\sum_\alpha e^{i\Phi^{ij}_\alpha}v^*_{\alpha,i}v_{\alpha,j}\right|^2 + J_2\sum_{\langle\langle i,j\rangle\rangle}|\boldsymbol{v}_i^*\cdot\boldsymbol{v}_j|^2. \tag{5}$$

Since $J_1, J_2 > 0$, the energy of each second-NN bond is minimized when $\boldsymbol{v}_i$, $\boldsymbol{v}_j$ are orthogonal and it is minimized for each first-NN bond when $|\sum_\alpha e^{i\Phi^{ij}_\alpha}v^*_{\alpha,i}v_{\alpha,j}| = 0$. Notably, we find that for all the first- and second-NN bonds and all values of valley-contrasting flux the conditions are satisfied by the spin-valley density wave ground state shown in Fig. 2. Three remarks are in order:

(1) The ground state for our two-orbital model exhibits *four*-sublattice spin-valley density wave order, a triplet-Q state with the commensurate wavevector ΓM. The situation is thus markedly different from the SU(2) Heisenberg model on the triangular lattice[42–44] for which the ground state for small J_2/J_1 is the 120°-state with *three*-sublattice order at the wavevector ΓK.

(2) The presence of the valley-contrasting flux affects the ground state manifold: If $\Phi^{ij}_\alpha = 0$, all semiclassical ground states have mutually orthogonal states on first-NN and second-NN bonds and can be generated from the configuration in Fig. 2 by a global SU(4) rotation.[45] If $\Phi^{ij}_\alpha \neq 0$ only a subset of these states, generated from the configuration in Fig. 2 by SU(2)×SU(2) rotations, are semiclassical ground states. For example, $\boldsymbol{v}_i = (1,0,1,0)^T$ and $\boldsymbol{v}_j = (1,0,-1,0)^T$ do not minimize the semiclassical energy of an first-NN bond if $\Phi^{ij}_\alpha \neq 0$ despite being mutually orthogonal. The manifold of ground states we found for $\Phi^{ij}_\alpha \neq 0$ is parameterized by two *independent* unit vectors denoting the spin axis associated with each valley.

(3) In addition to breaking the spin rotation symmetry from SU(2)×SU(2) to U(1)×U(1), the spin-valley density wave state breaks lattice translation symmetry. However, it preserves the U(1) valley number symmetry and, in particular, is valley-unpolarized. Our ground state has a finite energy gap to all excitations with an unbalanced occupation of the two valleys.

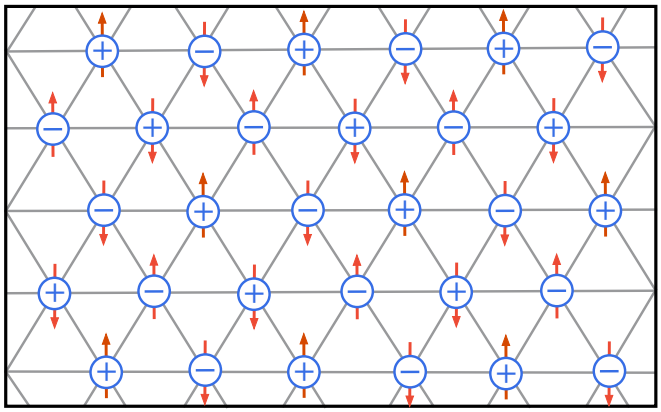

FIG. 2. (Color online) Spin-valley density wave with a four-sublattice order which is a variational ground state for all values of valley-contrasting flux Φ_α. The spin $\uparrow,\downarrow$-states are shown in red and the orbital $\pm$-states are shown in blue.

IV. QUANTUM FLUCTUATIONS

To understand the stability for the spin-valley density wave ground state of Fig. 2, we now proceed by studying the effects of quantum fluctuations with a generalized Holstein-Primakoff (HP) transformation.[46–48] We, therefore, assign the α-spin-orbital basis state to each site of the Λ_α-sublattice. Based on this choice, the generalized HP transformation for a site $i\in\Lambda_\alpha$ is given by $T^\alpha_{\alpha,i} = M - \sum_{\beta\neq\alpha} b^{\alpha\dagger}_{\beta,i}b^\alpha_{\beta,i}$, $T^\alpha_{\beta,i} = b^{\alpha\dagger}_{\beta,i}(M - \sum_{\beta\neq\alpha} b^{\alpha\dagger}_{\beta,i}b^\alpha_{\beta,i})^{1/2}$, $T^\beta_{\alpha,i} = (M - \sum_{\beta\neq\alpha} b^{\alpha\dagger}_{\beta,i}b^\alpha_{\beta,i})^{1/2}b^\alpha_{\beta,i}$ and $T^{\beta'}_{\beta,i} = b^{\alpha\dagger}_{\beta,i}b^\alpha_{\beta',i}$ where $b^\alpha_{\beta,i}$ denote bosonic operators with $\beta\neq\alpha$ and M is a positive integer. Next, we insert the HP transformation in the effective Hamiltonian of Eq. (3), perform a $1/M$-expansion, and only retain terms that are quadratic in the bosonic operators. The exchange interaction then takes on the form $H_J \approx M\sum_{\alpha\neq\beta}H_{\alpha\beta}$ where

$$H_{\alpha\beta} = J_1\sum_{\substack{\langle i,j\rangle\\ i\in\Lambda_\alpha, j\in\Lambda_\beta}} A^\dagger_{ij}A_{ij} + J_2\sum_{\substack{\langle\langle i,j\rangle\rangle\\ i\in\Lambda_\alpha, j\in\Lambda_\beta}} B^\dagger_{ij}B_{ij}, \tag{6}$$

and we have introduced the bond-operators $A^\dagger_{ij} = e^{i\Phi^{ij}_\beta}b^{\beta\dagger}_{\alpha,j} + e^{i\Phi^{ij}_\alpha}b^\alpha_{\beta,i}$ and $B^\dagger_{ij} = b^{\beta\dagger}_{\alpha,j} + b^\alpha_{\beta,i}$. In this representation of the effective Hamiltonian, b^β_α only pairs with b^α_β which implies that that individual $H_{\alpha\beta}$-terms decouple and can, thus, be studied independently of each other. For deriving the aforementioned stability phase diagram, we proceed in two steps:

First, as shown in Appendix C, we Fourier transform the Hamiltonian of Eq. (6) to momentum space and diagonalize it by means of a Bogoliubov transformation. This gives the dispersions,

$$\omega^{\alpha\beta}_{\mathbf{k}} = 2(J_1+J_2)\sqrt{1-|\gamma^{\alpha\beta}_{\mathbf{k}}|^2}, \tag{7}$$

where $\mathbf{k}$ is a momentum in the reduced Brillouin zone (RBZ) of the four-sublattice ordered spin-valley density wave state. Moreover, we defined the factor $\gamma_{\mathbf{k}}^{\alpha\beta} = [J_1 \cos(\mathbf{k}\cdot\mathbf{R}_{\alpha\beta}^{(1)} + \Phi_\alpha - \Phi_\beta) + J_2 \cos(\mathbf{k}\cdot\mathbf{R}_{\alpha\beta}^{(2)})]/(J_1+J_2)$. Here, $\mathbf{R}_{\alpha\beta}^{(1)}$ is a vector that connects the first-NN sites of the Λ_α- and Λ_β-sublattices and points along the bond direction. Similarly, $\mathbf{R}_{\alpha\beta}^{(2)}$ is a vector which connects the second-NN sites of the Λ_α- and Λ_β-sublattices. At this point, two comments are in order:

(1) If $J_2 = 0$, the dispersions vanish along the line $\mathbf{k}\cdot\mathbf{R}_{\alpha\beta}^{(1)} + \Phi_\alpha - \Phi_\beta = 0$ and we anticipate that the resulting low-energy quantum fluctuations destroy the spin-valley density wave order. This means that the spin-valley density wave order for TG/h-BN is not possible in previous models with $t_2 = 0$.[22–25]

(2) If $J_2 \neq 0$, the dispersion vanishes at discrete points in the RBZ. We expect that this behavior will reduce low-energy quantum fluctuations and will be crucial for stabilizing the spin-valley density wave order.

To confirm these arguments, we compute the reduction of the α-ordered moment due to the quantum fluctuations, $\langle T_{\alpha,i}^{\alpha}\rangle = M - \langle \sum_{\beta\neq\alpha} b_{\beta,i}^{\alpha\dagger} b_{\beta,i}^{\alpha}\rangle$ where the i-site is on the Λ_α-sublattice. We find that in momentum space,

$$\langle T_{\alpha,i}^{\alpha}\rangle = M - \frac{1}{2}\sum_{\beta\neq\alpha}\left\langle \frac{1}{\sqrt{1-|\gamma_{\mathbf{k}\tau}^{\alpha\beta}|^2}} - 1\right\rangle_{\mathrm{RBZ}}. \quad (8)$$

Here, $\langle ...\rangle_{\mathrm{RBZ}}$ denotes the average over the RBZ. By numerically evaluating Eq. (8) and setting $M = 1$, we find that $\langle T_{\alpha,i}^{\alpha}\rangle > 0$ for $J_2/J_1 \gtrapprox 0.12$, see Appendix C. This threshold does not depend on the orbital-contrasting flux as the latter only provides a constant momentum-space displacement in the dispersion of Eq. (7) and, thereby, does not change the RBZ-average. Accordingly, our prediction is that the system transitions from a disordered phase for $J_2/J_1 \lessapprox 0.12$ to a phase with a stable spin-valley density wave order for $J_2/J_1 \gtrapprox 0.12$. The nature of the disordered phase is an interesting question we leave to a separate study.

V. ZEEMAN FIELD EFFECTS

We will now study the effects of spin/orbital-Zeeman fields in our spin-orbital model,

$$H = H_J - h_\sigma \sum_i \sigma_i^z - h_\tau \sum_i \tau_i^z, \quad (9)$$

where σ and τ are 2×2 Pauli matrices acting in spin and orbital subspace respectively. In TG/h-BN, the spin-Zeeman field can be realized by an in-plane magnetic field and the valley-Zeeman field by an out-of-plane magnetic field.

First, we set the orbital-Zeeman field to zero, $h_\tau = 0$, and consider the case of a spin-Zeeman field h_σ. A large h_σ freezes the spin degrees of freedom and we can recast H_J into a form that includes only the remaining orbital degrees of freedoms. Neglecting the small J_2 term, we find that,

$$H \approx J_1 \sum_{\langle i,j\rangle} [1 + \boldsymbol{\tau}_i \cdot \boldsymbol{\Omega}_z(2\Phi^{ij})\cdot \boldsymbol{\tau}_j]/2. \quad (10)$$

Here, $\boldsymbol{\Omega}_z(\theta)$ is a rotation matrix about the z-axis by a θ-angle. Eq. (10) can also be written as an anisotropic exchange interaction with a Dzyaloshinskii-Moriya term, $\sim J_1[1+\tau_i^z\tau_j^z + \cos(2\Phi^{ij})(\tau_i^x\tau_j^x+\tau_i^y\tau_j^y) + \sin(2\Phi^{ij})(\tau_i^x\tau_j^y - \tau_i^y\tau_j^x)]/2$ with $\Phi^{ij} = -\Phi^{ji} = \Phi$.

To find the semiclassical ground state of Eq. (10), we minimize the expectation value of H with respect to the orientation of orbital pseudospin $\vec{\tau}$ at every site. Here, we will focus on a particular case when the lower energy bound $E_{ij} \geq J_1(1-S^2)/2$ is saturated for all bonds. Such a situation is achieved for $\Phi = \pi/6$ and, in this case, we find that the unique ground state is the 120° planar spin state, where spins lie on the xy plane. Since the 120°-state has three-sublattice order distinct from the four-sublattice order of the spin-valley density wave state at zero Zeeman field, we predict that by increasing the spin Zeeman field in TG/h-BN a phase transition between insulating states with different spin-valley density wave orders can be achieved.

Next, we set the spin-Zeeman field to zero, $h_\sigma = 0$, and consider a finite valley-Zeeman field h_τ. Since our ground state preserves the valley $U(1)$ symmetry and has a gap to valley excitations, we expect that the ground state is unchanged by a small valley Zeeman field. However, for a strong valley-Zeeman field, the system can lower its energy by aligning orbital pseudospins in the same direction, thus, effectively freezing the orbital degrees of freedom. We are then left with a $J_1 - J_2$ Heisenberg model of spins on a triangular lattice for which the three-sublattice ordered 120°-state is the semiclassical ground state when $J_2/J_1 \ll 1$.

For both spin and valley Zeeman fields, the spin-valley density wave state at zero/small field and the polarized state at high-field have distinct symmetries, and hence, must be separated by phase transitions.

VI. THERMAL MELTING

Finally, we discuss the effect of thermal fluctuations. Since the spin-valley density wave ground state breaks spin rotation symmetry, at finite temperature long-range order is destroyed by thermal fluctuations associated with Goldstone modes. However, a partially ordered state with composite order parameters that only break discrete symmetries may exist at low temperature. One such state is a unidirectional valley density wave (or valley stripe) at wavevector ΓM, in which spin order is restored but lattice translation symmetry is broken.

VII. CONCLUSION

We have introduced and studied a two-valley Hubbard model on a triangular lattice for describing the correlated insulator phases of TG/h-BN and twisted TMDs. Specifically, in the strong coupling limit, we have identified a four-sublattice ordered spin-valley density wave state as an ordered ground state that appears at moderate values of beyond-NN hoppings. Moreover, we have demonstrated that this spin-valley density wave-state undergoes a phase transition to a 120°-state in either spin- or orbital space upon increasing the magnitude of an external spin- or valley-Zeeman field.

ACKNOWLEDGMENTS

We would like to thank Zhen Bi, Noah F. Q. Yuan and Hiroki Isobe for helpful discussions. We also thank Feng Wang and Abhay Pasupathy for simulating discussions on trilayer graphene and twisted bilayer TMD, respectively. This work was supported by DOE Office of Basic Energy Sciences, Division of Materials Sciences and Engineering under Award DE-SC0018945. Liang Fu was supported in part by a Simons Investigator Award from the Simons Foundation.

Appendix A: Exchange interaction

In this first appendix, we will derive the effective exchange interaction between first and second-nearest sites as given in Eq. (3) of the main text. As a starting point, we note that to second order in t_1, t_2, the general form of the effective Hamiltonian is given by

$$H_J = -\frac{PH_0(1-P)H_0P}{H_I - E_0}, \tag{A1}$$

Here, we have introduced the operator P that projects on the ground states at energy E_0 with all sites singly-occupied.

Next, we evaluate the effective Hamiltonian in Eq. (A1) by computing all possible sequences of intermediate states, see Fig. 3. More specifically, for a fixed $\langle i,j\rangle$-bond, an electron can hop from the j-site to the i-site and back,

$$\sum_{\alpha,\beta} P(e^{-i\Phi^{ij}_\alpha} c^\dagger_{j\alpha}c_{i\alpha})(e^{i\Phi^{ij}_\beta} c^\dagger_{i\beta}c_{j\beta})P = \sum_{\alpha,\beta}[1 - e^{i(\Phi^{ij}_\beta - \Phi^{ij}_\alpha)}P(c^\dagger_{i\beta}c_{i\alpha}c^\dagger_{j\alpha}c_{j\beta})P] = \sum_{\alpha,\beta}[1 - P(e^{i(\Phi^{ij}_\beta - \Phi^{ij}_\alpha)}T^\alpha_{\beta,i}T^\beta_{\alpha,j})P]. \tag{A2}$$

Alternatively, the electron can also hop from the i-site to the j-site and back,

$$\sum_{\alpha,\beta} P(e^{i\Phi^{ij}_\beta} c^\dagger_{i\beta}c_{j\beta})(e^{-i\Phi^{ij}_\alpha} c^\dagger_{j\alpha}c_{i\alpha})P = \sum_{\alpha,\beta}[1 - e^{i(\Phi^{ij}_\beta - \Phi^{ij}_\alpha)}P(c^\dagger_{i\beta}c_{i\alpha}c^\dagger_{j\alpha}c_{j\beta})P] = \sum_{\alpha,\beta}[1 - P(e^{i(\Phi^{ij}_\beta - \Phi^{ij}_\alpha)}T^\alpha_{\beta,i}T^\beta_{\alpha,j})P]. \tag{A3}$$

If we combine the two types of sequences, multiply by the appropriate energy denominator, and repeat these same steps for the $\langle\langle i,j\rangle\rangle$-bonds, we arrive at the effective exchange interaction,

$$H_J = J_1 \sum_{\langle i,j\rangle}\sum_{\alpha,\beta} e^{i(\Phi^{ij}_\beta - \Phi^{ij}_\alpha)}T^\alpha_{\beta,i}T^\beta_{\alpha,j} + J_2 \sum_{\langle\langle i,j\rangle\rangle}\sum_{\alpha,\beta} T^\alpha_{\beta,i}T^\beta_{\alpha,j}. \tag{A4}$$

Because of the α,β-summation, we note that this expression for H_J is invariant under a swapping the $\langle i,j\rangle$-bond indices or, equivalently, reversing the $\langle i,j\rangle$-bond direction. In particular, this means that the $\langle i,j\rangle$-summation in H_J does not require us to consider directed bonds as in the case of H_0.

Appendix B: Minimization condition

In this second appendix, we provide more details on the derivation of the minimization condition given in Eq. (5) of the main text. More specifically, we will focus on deriving the first term $\propto J_1$.

As a first step, we consider a fixed $\langle i,j\rangle$-bond and notice that the action of H_J on this bond is given by

$$H_{ij} \equiv \sum_{\alpha,\beta} e^{i(\Phi^{ij}_\beta - \Phi^{ij}_\alpha)}T^\alpha_{\beta,i}T^\beta_{\alpha,j} = \sum_{\alpha,\beta} e^{i(\Phi^{ij}_\beta - \Phi^{ij}_\alpha)}|\beta_i,\alpha_j\rangle\langle\alpha_i,\beta_j|. \tag{B1}$$

As a second step, we consider a state of the $\langle i,j\rangle$-bond we will assume to be product state in bond space,

$$\boldsymbol{v}_{ij} = \left(\sum_{\alpha} v_{\alpha,i}\,|\alpha\rangle_i\right)\left(\sum_{\beta} v_{\beta,j}\,|\beta\rangle_j\right) = \sum_{\alpha,\beta} v_{\alpha,i}\,v_{\beta,j}\,|\alpha_i,\beta_j\rangle \tag{B2}$$

As a final step, we evaluate the expression,

$$\begin{aligned}
\boldsymbol{v}_{ij}^{\dagger}\cdot H_{ij}\cdot\boldsymbol{v}_{ij} &= \sum_{\alpha,\beta}\sum_{\alpha',\beta'}\sum_{\alpha'',\beta''} e^{i(\Phi^{ij}_{\beta''}-\Phi^{ij}_{\alpha''})} v^{*}_{\alpha',i}\,v^{*}_{\beta',j}v_{\alpha,i}\,v_{\beta,j}\,\langle\alpha'_i,\beta'_j|\,\beta''_i,\alpha''_j\rangle\langle\alpha''_i,\beta''_j\,|\alpha_i,\beta_j\rangle \\
&= \sum_{\alpha,\beta}\sum_{\alpha',\beta'}\sum_{\alpha'',\beta''} e^{i(\Phi^{ij}_{\beta''}-\Phi^{ij}_{\alpha''})}\; v^{*}_{\alpha',i}\,v^{*}_{\beta',j}v_{\alpha,i}\,v_{\beta,j}\;\delta_{\alpha'\beta''}\delta_{\beta'\alpha''}\delta_{\alpha'',\alpha}\delta_{\beta'',\beta} \\
&= \sum_{\alpha,\beta} e^{i(\Phi^{ij}_{\beta}-\Phi^{ij}_{\alpha})}\; v^{*}_{\beta,i}\,v^{*}_{\alpha,j}v_{\alpha,i}\,v_{\beta,j} \\
&= \left(\sum_{\alpha} e^{-i\Phi^{ij}_{\alpha}}\,v_{\alpha,i}v^{*}_{\alpha,j}\right)\left(\sum_{\beta} e^{i\Phi^{ij}_{\beta}}\,v^{*}_{\beta,i}v_{\beta,j}\right) \\
&= \left|\sum_{\alpha} e^{i\Phi^{ij}_{\alpha}}\,v^{*}_{\alpha,i}v_{\alpha,j}\right|^2 .
\end{aligned} \tag{B3}$$

This result corresponds to the first term $\propto J_1$ in Eq. (5) of the main text.

Appendix C: Dispersion relations

In this third Appendix, we consider in more detail the derivation of the dispersion relations given by Eq. (7) in the main text. For clarity, we will initially set $J_2 = 0$ in our derivation.

First, we perform a generalized Holstein-Primakoff transformation as described in the main text. If we only retain terms that are quadratic in the bosonic operators, we find that $H_J \approx M\sum_{\alpha\neq\beta} H_{\alpha\beta}$ with,

$$H_{\alpha\beta} = J_1 \sum_{\substack{\langle i,j\rangle \\ i\in\Lambda_\alpha, j\in\Lambda_\beta}} b^{\alpha\dagger}_{\beta,i}b^{\alpha}_{\beta,i} + b^{\beta\dagger}_{\alpha,j}b^{\beta}_{\alpha,j} + e^{i(\Phi^{ij}_{\beta}-\Phi^{ij}_{\alpha})}b^{\alpha\dagger}_{\beta,i}b^{\beta\dagger}_{\alpha,j} + e^{-i(\Phi^{ij}_{\beta}-\Phi^{ij}_{\alpha})}b^{\alpha}_{\beta,i}b^{\beta}_{\alpha,j}. \tag{C1}$$

In the following considerations, we define $\boldsymbol{\delta}_j$ $(j = 1, ..., 3)$ to be lattice basis vectors pointing along the directed bonds of the triangular lattice and, as a result of rotational symmetry, we have $e^{i\Phi^{\mathbf{r},\mathbf{r}+\boldsymbol{\delta}_j}_{\alpha}} = e^{i\Phi_\alpha}$.

Second, we consider sites $\mathbf{r}\in\Lambda_\alpha$ with nearest-neighbors $\mathbf{r}\pm\boldsymbol{\delta}\in\Lambda_\beta$. Then we can rewrite $H_{\alpha\beta}$ as,

$$\begin{aligned}
H_{\alpha\beta} &= J_1\sum_{\mathbf{r}}\left[2b^{\alpha\dagger}_{\beta,\mathbf{r}}b^{\alpha}_{\beta,\mathbf{r}} + b^{\beta\dagger}_{\alpha,\mathbf{r}-\boldsymbol{\delta}}b^{\beta}_{\alpha,\mathbf{r}-\boldsymbol{\delta}} + b^{\beta\dagger}_{\alpha,\mathbf{r}+\boldsymbol{\delta}}b^{\beta}_{\alpha,\mathbf{r}+\boldsymbol{\delta}}\right] \\
&\quad + J_1\sum_{\mathbf{r}}\left[e^{i(\Phi^{\mathbf{r},\mathbf{r}-\delta}_{\beta}-\Phi^{\mathbf{r},\mathbf{r}-\delta}_{\alpha})}b^{\alpha\dagger}_{\beta,\mathbf{r}}b^{\beta\dagger}_{\alpha,\mathbf{r}-\boldsymbol{\delta}} + e^{i(\Phi^{\mathbf{r},\mathbf{r}+\boldsymbol{\delta}}_{\beta}-\Phi^{\mathbf{r},\mathbf{r}+\boldsymbol{\delta}}_{\alpha})}b^{\alpha\dagger}_{\beta,\mathbf{r}}b^{\beta\dagger}_{\alpha,\mathbf{r}+\boldsymbol{\delta}} + \text{H.c.}\right]
\end{aligned} \tag{C2}$$

By lattice translation symmetry, we have $e^{i\Phi^{\mathbf{r},\mathbf{r}+\boldsymbol{\delta}}_{\alpha}} = e^{i\Phi^{\mathbf{r}-\boldsymbol{\delta},\mathbf{r}}_{\alpha}} = e^{-i\Phi^{\mathbf{r},\mathbf{r}-\boldsymbol{\delta}}_{\alpha}}$. This implies,

$$\begin{aligned}
H_{\alpha\beta} &= J_1\sum_{\mathbf{r}}\left[2b^{\alpha\dagger}_{\beta,\mathbf{r}}b^{\alpha}_{\beta,\mathbf{r}} + b^{\beta\dagger}_{\alpha,\mathbf{r}-\boldsymbol{\delta}}b^{\beta}_{\alpha,\mathbf{r}-\boldsymbol{\delta}} + b^{\beta\dagger}_{\alpha,\mathbf{r}+\boldsymbol{\delta}}b^{\beta}_{\alpha,\mathbf{r}+\boldsymbol{\delta}}\right] \\
&\quad + J_1\sum_{\mathbf{r}}\left[e^{-i(\Phi^{\mathbf{r},\mathbf{r}+\delta}_{\beta}-\Phi^{\mathbf{r},\mathbf{r}+\delta}_{\alpha})}b^{\alpha\dagger}_{\beta,\mathbf{r}}b^{\beta\dagger}_{\alpha,\mathbf{r}-\boldsymbol{\delta}} + e^{i(\Phi^{\mathbf{r},\mathbf{r}+\delta}_{\beta}-\Phi^{\mathbf{r},\mathbf{r}+\delta}_{\alpha})}b^{\alpha\dagger}_{\beta,\mathbf{r}}b^{\beta\dagger}_{\alpha,\mathbf{r}+\boldsymbol{\delta}} + \text{H.c.}\right]
\end{aligned} \tag{C3}$$

Third, we define the Fourier transforms, $b^{\alpha}_{\beta,\mathbf{r}} = (N/4)^{-1/2}\sum_{\mathbf{k}\in\text{RBZ}} b^{\alpha}_{\beta,\mathbf{k}}e^{i\mathbf{k}\cdot\mathbf{r}}$ where the site $\mathbf{r}$ is on the Λ_α-sublattice. Moreover, N is the number of lattice unit cells and $\mathbf{k}$ is a momentum in the reduced Brillouin zone of the four-sublattice ordered spin-valley density wave state. We now rewrite the Hamiltonian as,

$$H_{\alpha\beta} = 2J_1\sum_{\mathbf{k}\in\text{RBZ}}\left[b^{\beta\dagger}_{\alpha,\mathbf{k}}b^{\beta}_{\alpha,\mathbf{k}} + b^{\alpha\dagger}_{\beta,-\mathbf{k}}b^{\alpha}_{\beta,-\mathbf{k}} + \gamma^{\alpha\beta}_{\mathbf{k}}b^{\alpha\dagger}_{\beta,-\mathbf{k}}b^{\beta\dagger}_{\alpha,\mathbf{k}} + (\gamma^{\alpha\beta}_{\mathbf{k}})^{*}b^{\alpha}_{\beta,-\mathbf{k}}b^{\beta}_{\alpha,\mathbf{k}}\right], \tag{C4}$$

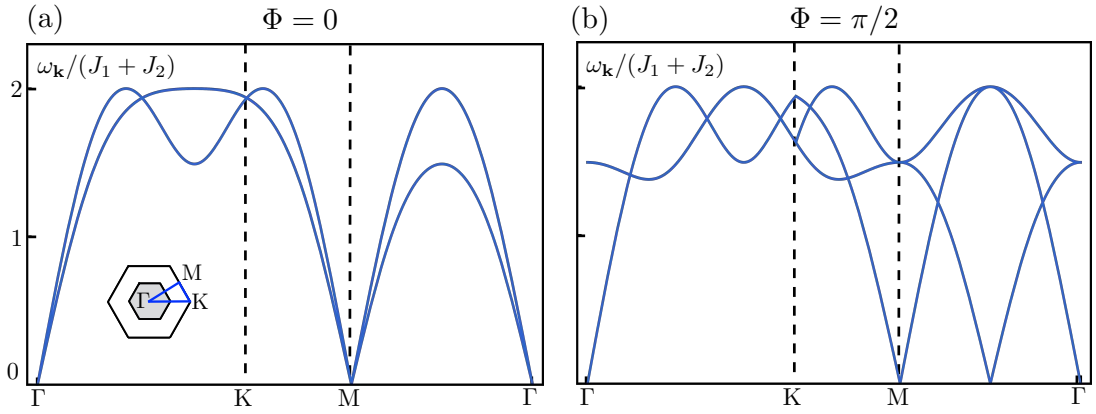

FIG. 3. (Color online) (a) Plot of the dispersions relations of Eq. 26 along the high-symmetry lines of the Brillouin zone for $\Phi = 0$ and $J_2/J_1 = 0.2$. Inset: Brillouin zone of the triangular lattice (white) and structural Brillouin of the four-sublattice spin-valley density wave state (gray). (b) Same as (a) but for $\Phi = \pi/2$.

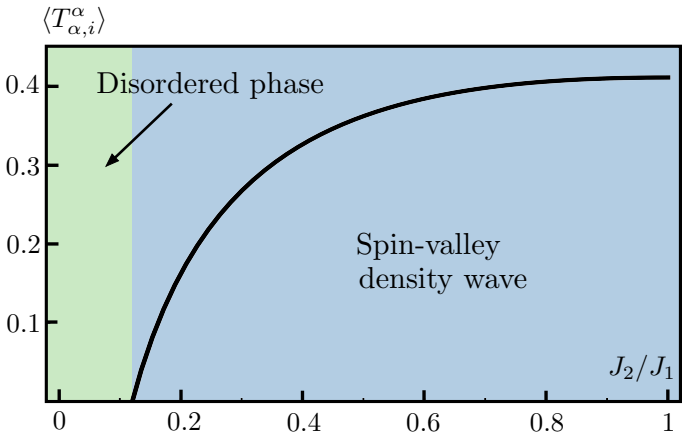

FIG. 4. (Color online) Plot of the ordered moment as a function of J_2/J_1. We find that $\langle T^{\alpha}_{\alpha,i} \rangle > 0$ for $J_2/J_1 \gtrapprox 0.12$ which implies that the spin-valley density wave order is stabilized in this regime (shown in green). If $J_2/J_1 \lessapprox 0.12$, the spin-valley density wave ordered is destroyed by low-energy quantum fluctuations and the system is in a disordered phase. These results are independent of the value of valley contrasting flux.

where we have introduced the factor,

$$\gamma^{\alpha\beta}_{\mathbf{k}} = \cos(\mathbf{k}\cdot\boldsymbol{\delta} + \Phi_\alpha - \Phi_\beta) \tag{C5}$$

Fourth, we allow for $J_2 \neq 0$ which amounts to replacements,

$$H_{\alpha\beta} \to 2(J_1+J_2) \sum_{\mathbf{k}\in \mathrm{RBZ}} \left[b^{\beta\dagger}_{\alpha,\mathbf{k}} b^{\beta}_{\alpha,\mathbf{k}} + b^{\alpha\dagger}_{\beta,-\mathbf{k}} b^{\alpha}_{\beta,-\mathbf{k}} + \gamma^{\alpha\beta}_{\mathbf{k}} b^{\alpha\dagger}_{\beta,-\mathbf{k}} b^{\beta\dagger}_{\alpha,\mathbf{k}} + (\gamma^{\alpha\beta}_{\mathbf{k}})^* b^{\alpha}_{\beta,-\mathbf{k}} b^{\beta}_{\alpha,\mathbf{k}} \right], \tag{C6}$$

$$\gamma^{\alpha\beta}_{\mathbf{k}} \to [J_1 \cos(\mathbf{k}\cdot\mathbf{R}^{(1)}_{\alpha\beta} + \Phi_\alpha - \Phi_\beta) + J_2 \cos(\mathbf{k}\cdot\mathbf{R}^{(2)}_{\alpha\beta})]/(J_1+J_2) \tag{C7}$$

Here, we have also replaced $\boldsymbol{\delta} \to \mathbf{r}^{(1)}_{\alpha\beta}$ and $\mathbf{r}^{(2)}_{\alpha\beta}$ is a vector that connects the second nearest-neighbor sites of the Λ_α- and Λ_β-sublattices.

Finally, by performing a Bogoliubov transformation, we arrive at the dispersions

$$\omega^{\alpha\beta}_{\mathbf{k}} = 2(J_1+J_2)\sqrt{1-|\gamma^{\alpha\beta}_{\mathbf{k}}|^2}. \tag{C8}$$

This concludes the derivation.

[1] R. Bistritzer and A. MacDonald, Proc. Natl. Acad. Sci. **108**, 12233 (2011).
[2] G. TramblydeLaissardiere, D. Mayou, and L. Magaud, Phys. Rev. B **86**, 125413 (2012).
[3] Y. Cao, V. Fatemi, A. Demir, S. Fang, S. L. Tomarken, J. Y. Luo, J. D. Sanchez-Yamagishi, K. Watanabe, T. Taniguchi, E. Kaxiras, R. C. Ashoori, and P. Jarillo-Herrero, Nature **556**, 80 (2018).
[4] Y. Cao, V. Fatemi, S. Fang, K. Watanabe, T. Taniguchi, E. Kaxiras, and P. Jarillo-Herrero, Nature **556**, 43 (2018).
[5] A. Kerelsky, L. McGilly, D. M. Kennes, L. Xian, M. Yankowitz, S. Chen, K. Watanabe, T. Taniguchi, J. Hone, C. Dean, A. Rubio, and A. N. Pasupathy, arXiv:1812.08776 (2018).
[6] Y. Choi, J. Kemmer, Y. Peng, A. Thomson, H. Arora, R. Polski, Y. Zhang, H. Ren, J. Alicea, G. Refael, F. von Oppen, K. Watanabe, T. Taniguchi, and S. Nadj-Perge, arXiv:1901.02997 (2019).
[7] M. Yankowitz, S. Chen, H. Polshyn, K. Watanabe, T. Taniguchi, D. Graf, A. F. Young, and C. R. Dean, Science 10.1126/science.aav1910 (2019).
[8] Y. Cao, D. Chowdhury, D. Rodan-Legrain, O. Rubies-Bigordà, K. Watanabe, T. Taniguchi, T. Senthil, P. Jarillo-Herrero, arXiv:1901.03710 (2019).
[9] A. L. Sharpe, E. J. Fox, A. W. Barnard, J. Finney, K. Watanabe, T. Taniguchi, M. A. Kastner, D. Goldhaber-Gordon, arXiv:1901.03520 (2019).
[10] G. Chen, L. Jiang, S. Wu, B. Lv, H. Li, K. Watanabe, T. Taniguchi, Z. Shi, Y. Zhang, and F. Wang, arXiv:1803.01985 (2018).
[11] G. Chen, A. L. Sharpe, P. Gallagher, I. T. Rosen, E. Fox, L. Jiang, B. Lyu, H. Li, K. Watanabe, T. Taniguchi, J. Jung, Z. Shi, D. Goldhaber-Gordon, Y. Zhang, and F. Wang, arXiv:1901.04621 (2019).
[12] G. Chen, A. L. Sharpe, E. J. Fox, Y.-H. Zhang, S. Wang, L. Jiang, B. Lyu, H. Li, K. Watanabe, T. Taniguchi, Z. Shi, T. Senthil, D. Goldhaber-Gordon, Y. Zhang, and F. Wang, arXiv:1905.06535 (2019).
[13] E-M. Shih, L. Wang, A. Ghiotto, D. Rhodes, C. Tan, J. Hone, A. N. Pasupathy, and C. R. Dean, GrapheneUS: Graphene & 2D Materials International Conference and Exhibition, Poster presentation (2019).
[14] L. Jauregui, K. Pistunova, A. Y. Joe, D. Rhodes, B. Kim, J. Hone, and P. Kim, APS March Meeting 2019, Abstract: K15.00003 (2019).
[15] C. Xu and L. Balents, Phys. Rev. Lett. **121**, 087001 (2018).
[16] X.-C. Wu, A. Keselman, C.-M. Jian, K. A. Pawlak, and C. Xu, arXiv:1905.00033 (2019).
[17] N. F. Q. Yuan and L. Fu, Phys. Rev. B **98**, 045103 (2018).
[18] M. Koshino, N. F. Q. Yuan, T. Koretsune, M. Ochi, K. Kuroki, and L. Fu, Phys. Rev. X **8**, 031087 (2018).
[19] F. Wu, T. Lovorn, E. Tutuc, and A. H. MacDonald, Phys. Rev. Lett. **121**, 026402 (2018).
[20] F. Wu, T. Lovorn, E. Tutuc, I. Martin, and A. H. MacDonald, Phys. Rev. Lett. **122**, 086402 (2019).
[21] M. Koshino and E. McCann, Phys. Rev. B **80**, 165409 (2009).
[22] H. C. Po, L. Zou, A. Vishwanath, and T. Senthil, Phys. Rev. X **8**, 031089 (2018).
[23] G.-Y. Zhu, T. Xiang, and G.-M. Zhang, Science Bulletin **63**, 1087 (2018).
[24] G.-Y. Zhu, T. Xiang, and G.-M. Zhang, arXiv:1806.07535 (2018).
[25] L. Classen, C. Honerkamp, and M. M. Scherer, arXiv:1902.05350 (2019).
[26] Y.-H. Zhang and T. Senthil, arXiv:1809.05110 (2018).
[27] B. L. Chittari, G. Chen, Y. Zhang, F. Wang, and J. Jung, Phys. Rev. Lett. **122**, 016401 (2019).
[28] Y.-H. Zhang, D. Mao, Y. Cao, P. Jarillo-Herrero, and T. Senthil, Phys. Rev. B **99**, 075127 (2019).
[29] J. Kang, O. Vafek, arXiv:1810.08642 (2018).
[30] F. Guinea, N. R. Walet, arXiv:1806.05990 (2018).
[31] J. Kang, O. Vafek, Phys. Rev. X **8**, 031088 (2018).
[32] J. C. W. Song, P. Samutpraphoot, and L. S. Levitov, Proceedings of the National Academy of Sciences **112**, 10879 (2015).
[33] N. F. Q. Yuan, H. Isobe, and L. Fu, arXiv:1901.05432 (2019).
[34] H. Isobe, N. F. Q. Yuan, and L. Fu, Phys. Rev. X **8**, 041041 (2018).
[35] C.-C. Liu, L.-D. Zhang, W.-Q. Chen, and F. Yang, Phys. Rev. Lett. **121**, 217001 (2018).
[36] E. Laksono, J. N. Leaw, A. Reaves, M. Singh, X. Wang, S. Adam, and X. Gu, Solid State Commun. **282**, 38 (2018).
[37] Y. Sherkunov and J. J. Betouras, Phys. Rev. B **98**, 205151 (2018).
[38] D. M. Kennes, J. Lischner, and C. Karrasch, Phys. Rev. B **98**, 241407(R) (2018).
[39] Y.-P. Lin and R. M. Nandkishore, Phys. Rev. B **98**, 214521 (2018).
[40] Y.-Z. You and A. Vishwanath, arXiv:1805.06867 (2018).
[41] J. Gonzalez and T. Stauber, Phys. Rev. Lett. **122**, 026801 (2019).
[42] Z. Zhu and S.R. White, Phys. Rev. B **92**, 041105(R) (2015).
[43] W.-J. Hu, S.-S. Gong, W. Zhu, and D.N. Sheng, Phys. Rev. B **92**, 140403(R) (2015).
[44] S.-S. Gong, W. Zhu, J.-X. Zhu, D. N. Sheng, and K. Yang, Phys. Rev. B **96**, 075116 (2017).
[45] K. Penc, M. Mambrini, P. Fazekas, and F. Mila, Phys. Rev. B 68, 012408 (2003).
[46] N. Papanicolaou, Nuclear Physics B **240**, 281 (1984).
[47] N. Papanicolaou, Nuclear Physics B **305**, 367 (1988).
[48] A. Joshi, M. Ma, F. Mila, D. N. Shi, and F. C. Zhang, Phys. Rev. B **60**, 6584 (1999).